Role of the medial part of the intraparietal sulcus in implementing movement direction

M. Davare [1], A. Zénon [1], G. Pourtois [2], M. Desmurget [3], E. Olivier [1]

1. Institute of Neuroscience, Laboratory of Neurophysiology, Université catholique de Louvain, Brussels, Belgium,
2. Department of Experimental Clinical and Health Psychology, University of Ghent, Belgium
3. Centre de Neurosciences Cognitives, CNRS, UMR 5229, Bron, France.

Abbreviated title: Role of mIPS in movement direction

Corresponding author:
Marco Davare,
Institute of Neuroscience,
Université catholique de Louvain,
53, Avenue Mounier
COSY- B1.53.04
Brussels, Belgium.
Tel: 00 32 27645444
Fax: 00 32 27645465
Email: mdavare@ion.ucl.ac.uk

Abstract

The contribution of the posterior parietal cortex (PPC) to visually-guided movements has been originally inferred from observations made in patients suffering from optic ataxia. Subsequent electrophysiological studies in monkeys and functional imaging data in humans have corroborated the key role played by the PPC in sensorimotor transformations underlying goal-directed movements, although the exact contribution of this structure remains debated. Here, we used transcranial magnetic stimulation (TMS) to interfere transiently with the function of the left or right medial part of the intraparietal sulcus (mIPS) in healthy volunteers performing visually-guided movements with the right hand. We found that a 'virtual lesion' of either mIPS increased the scattering in initial movement direction, leading to longer trajectory and prolonged movement time, but only when TMS was delivered 100-160 ms before movement onset and for movements directed towards contralateral targets. Control experiments showed that deficits in initial movement direction consequent to mIPS virtual lesions resulted from an inappropriate implementation of the motor command underlying the forthcoming movement and not from an inaccurate computation of the target localisation. The present study indicates that mIPS plays a causal role in implementing specifically the direction vector of visually-guided movements towards objects situated in the contralateral hemifield.

Keywords: hand, TMS, reaching, visuomotor, wrist.

Introduction

In humans, functional imaging studies have shown that several areas in the posterior parietal cortex (PPC) are active during visually-guided movements (Deiber et al. 1996; Connolly et al. 2003; Prado et al. 2005; Culham and Valyear 2006; Blangero et al. 2009; Filimon et al. 2009; Hinkley et al. 2009) and/or while performing on-line corrections of such movements (Desmurget et al. 2001). In particular, it has been suggested that posterior regions of the PPC (the superior parieto-occipital cortex, SPOC, and the posterior part of intraparietal sulcus, IPS) process the spatial location of the target whereas more rostral parietal regions along the IPS, namely the medial (mIPS) and anterior (aIPS) portions of the IPS may play a role in implementing the output vector underlying reach-to-grasp movements (Grefkes et al. 2004; Beurze et al. 2009; Blangero *et al.* 2009; Cavina-Pratesi et al. 2010). This conclusion about the contribution of mIPS to visually-guided movements is congruent with results from non-human primate experiments showing that cells in the anterior part of the medial intraparietal area (MIP), the putative homologue of mIPS in humans (Grefkes and Fink 2005), encode the arm movement direction in intrinsic (motor) coordinates (Eskandar and Assad 1999).

However, in both monkeys and humans, the role of the medial region of the IPS in reaching movements has only been inferred from correlative techniques and a formal demonstration that its reversible lesion during movement planning actually affects the implementation of the motor command of reaching movements is still lacking. To date, only a few studies have investigated the disruptive effects of TMS on the performance of reaching movements (Smyrnis et al. 2003; Vesia et al. 2006; Vesia et al. 2008; Vesia et al. 2010). However, probably because these studies have used different tasks and targeted distinct

PPC regions, their conclusions remain discrepant. Whereas Smyrnis et al. (2003) showed that TMS applied over the left PPC disrupts the encoding of the target location in both visual hemifields at an early stage of the visuomotor transformation, Vesia et al. (2006, 2008 and 2010) concluded that the PPC involvement occurs downstream to the target representation process, possibly encoding the motor vector of the appropriate reaching movement.

In order to investigate the precise role of mIPS in planning visually-guided movements, we used single pulse TMS to induce transient virtual lesions of either the left or right mIPS in healthy subjects performing step-tracking movements with their right wrist. Instead of using a whole-arm reaching task, we chose to focus on a two degrees of freedom wrist movement task for two main reasons. First, the kinematics and pattern of muscle recruitment of these wrist movements have already been investigated in great details in healthy volunteers by Strick and collaborators (Hoffman and Strick 1999), which will facilitate the interpretation of our behavioural and EMG data. Second, the neural network underlying the execution of comparable two-dimensional movements has already been studied by using fMRI (Grefkes *et al.* 2004; Grefkes and Fink 2005), allowing direct comparison between our data and previous observations. Apart from these points, one may also notice that wrist rotation is a fundamental parameter during whole arm transport and it has been recently shown that a similar area encodes wrist rotation and whole-arm reaching movements (Fattori et al. 2009).

In the main experiment (Experiment #1), we explored the consequence of mIPS virtual lesions when occurring during the preparation of visually-guided movements. In a first control experiment (Experiment #2), we further investigated whether mIPS is involved in

coding the amplitude of goal-directed movements. Then, in two subsequent control experiments, we tested whether the deficits in initial movement direction found in Experiment #1 following mIPS virtual lesions could result from an inaccurate computation of the target position (Experiment #3) or from an incorrect outcome of the sensorimotor transformations (Experiment #4).

Materials and methods

Subjects

Twenty-three healthy subjects participated in the present study (mean age: 26.4±5.1 years). They were all right handed (Oldfield 1971), with normal, or corrected to normal, vision and gave their informed consent. None had a history of neurological disease. Potential risks of adverse reactions to TMS were evaluated by means of the TMS Adult Safety Screen questionnaire (Keel et al. 2001). None of the subjects had unexpected reactions to TMS. The present experiment was approved by the local ethical committee of the Université catholique de Louvain.

Experimental setup

Subjects sat comfortably in front of a 17-inch computer screen located at a distance of 65 cm. Their right forearm was fastened midway between pronation and supination and the right hand was used to grasp the handle of a two-axis manipulandum (Fig. 1A) (Hoffman and Strick 1986; Davare et al. 2007a). Two potentiometers placed on each axis of the manipulandum allowed us to measure the wrist displacements in the horizontal (flexion-extension [FE]) and vertical (radial-ulnar [RU]) planes, respectively. Feedback of the manipulandum position (4 mm yellow circle, 0.4 deg of visual angle) was continuously displayed on the screen.

Transcranial magnetic stimulation

Single-pulse TMS was delivered through a 70 mm figure-of-eight coil connected to a Magstim 200 stimulator (Magstim, Whitland, UK). Before each experiment, the resting motor threshold - defined as the minimum intensity that induced motor evoked potentials (MEPs) $\geq$50 μV peak-to-peak in the first dorsal interosseus (1DI) in 5 of 10 trials - was estimated for each subject. TMS intensity was then set at 120 % of the resting motor threshold for the whole experimental session.

In the present study, the coil was positioned, with the handle pointing downwards and perpendicular to the intraparietal sulcus, either over the left or the right mIPS by using a neuronavigation technique. This allowed us to project the centre of the coil to the brain surface reconstructed from a 3D structural MRI (Fig. 1D) (Noirhomme et al. 2004; Davare et al. 2006). In order to guide neuronavigation, the coil was first positioned over the medial portion of the intraparietal sulcus, near the caudal part of the angular gyrus. In a second step, the coil position was further adjusted so that the stimulation coordinates corresponded to the foci of activation found in the intraparietal sulcus during a similar task (MNI coordinates: -28, -50, 52 and 28, -56, 50 for the left and right mIPS, respectively) (Grefkes *et al.* 2004). In the present study, the mean normalized MNI coordinates ($\pm$SD) of the stimulation points were -32$\pm$5, -49$\pm$6 and 46$\pm$9 mm for the left mIPS and 33$\pm$5, -46$\pm$7 and 49$\pm$10 mm for the right mIPS (x,y,z), consistent with the location of the mIPS reported in studies using various approaches (see Table 1). It is noteworthy that our mIPS site is more anterior and lateral than the mIPS location used in another recent TMS study (Vesia et al., 2010). Interestingly, Striemer et al. (2011) also found a TMS effect similar to Vesia et al. (2010) over a more anterior site, closer to our coordinates. Moreover, our neuronavigation system projects the centre of the TMS coil onto the reconstructed cortical

mesh and since we were targeting a sulcus, our mIPS coordinates are found in the depth of the intraparietal sulcus; it is however more likely that we stimulated the part of mIPS on the cortical convexity. Participants wore a tight-fitting EEG cap, on which TMS sites were marked. A chin rest was also used to minimize head movements. Because the coil position changed in each block (left versus right hemisphere and sham versus normal position) and because of the short duration of each block, the coil was held by the experimenter.

The control condition was a sham TMS stimulation delivered over the same sites but with the coil held perpendicular to the scalp surface.

Experimental procedure

Each trial started with the wrist positioned midway between pronation and supination, a condition fulfilled when the position signal of the manipulandum (yellow circle) was positioned at the centre of the screen, indicated by a 17 mm (1.6 deg.) blue square. Subjects were instructed to fixate this square throughout the trial. After a 700 ms delay, this central square was turned off and a 17 mm red square target was turned on in one of the four corners of the screen (45, 135, 225 and 315 deg) at a retinal eccentricity of 7 deg. The amplitude of the wrist movement needed to capture these targets was 20 deg (Fig. 1B). Subjects were instructed to perform the movements as rapidly and as accurately as possible and to keep the cursor inside the target for at least 700 ms. Inter-trial interval varied randomly from 3.5 to 5 seconds.

Experiment #1. Nine subjects (mean age: 25.3±4.2 years) participated in the main experiment which consisted of eight blocks of 40 trials each. TMS was applied either over

left mIPS (2 blocks) or right mIPS (2 blocks) and delivered either 100 or 200 ms after target presentation; these two timings were selected to investigate the whole movement preparation period, taking advantage of the normal variability in reaction time (see 'Data acquisition and analysis'). Four additional blocks were gathered with the coil in the sham position, also located either over left mIPS (2 blocks) or right mIPS (2 blocks). Targets appeared randomly and the order of the 8 blocks was pseudo-randomly counterbalanced across subjects.

Experiment #2. In this first control experiment we tested whether the absence of TMS-induced deficits on movement amplitude (see Results of Experiment #1) could be explained by the fact that the target eccentricity remained constant. To address this question, 6 new subjects (mean age: 26.7±5.8 years) performed an experiment in which targets were displayed in the same 4 directions as in Experiment #1 but at 3 different retinal eccentricities, namely 3.5, 5.25 or 7 deg, corresponding, respectively, to a wrist movement amplitude of 10, 15 or 20 deg. In this control experiment, we performed 6 blocks of 120 trials (2 blocks with TMS delivered over left mIPS, 2 TMS blocks over right mIPS and 2 sham blocks, one over each mIPS). As in Experiment #1, single pulse TMS was delivered during movement preparation, 100 or 200 ms after target display. In addition, in this experiment, eye position was monitored by means of an infrared camera (Thomas Recordings, Giessen, Germany) connected to a data acquisition card (National Instruments, Austin, TX) on a personal computer. This was done to rule out the possibility that specific effects of the TMS on eye movements could have explained the results of Experiment #1.

Experiment #3. This second control experiment aimed to test whether the TMS-induced deficits found in visually-directed movements (see Results, Experiment #1) could be

explained by an inaccurate computation of the target position. To test this hypothesis, we used a delayed match-to-sample paradigm in 8 additional subjects (mean age: 28.1±5.1 years). In this experiment, the subjects had to fixate a cross located at the centre of the screen. Next, a target (same location as targets 1 and 4 in Experiment #1 and at a constant eccentricity of 7 deg, see Fig. 1) was presented for 500 ms either in the right or left upper hemifield. Then, following the display of a half-screen mask for 500 ms (red noise over black background in the upper visual field), a second target was displayed in the same hemifield and at the same eccentricity but in a slightly different direction with respect to the first target (left or right shift of 2, 4 or 8 deg). Randomly in one out of 7 trials, the second target appeared at the exact same location as the first one. The task consisted of pressing the right or left arrow key on a computer keyboard to indicate whether the second target shifted clockwise or anti-clockwise, respectively, in comparison with the first target. The eye position was controlled throughout the experiment using an EyeLink camera (SR research, Ottawa, Canada) connected to a computer; if subjects broke fixation, the trial was aborted and repeated later (this happened in less than 4% of the trials and occurred randomly across experimental conditions). A pilot study performed on 4 subjects and using 6 possible shift sizes (±2, 4, 6, 8, 10 or 12 deg with respect to the first target) allowed us to determine the optimal amplitude of the second target shift, i.e. the shift size for which the probability of correct responses was 90, 75 and 65%. TMS was delivered either 160 or 200 ms after the first target display. These two delays were used because, in Experiment #1, TMS-induced effects were only significant in a 100-160 ms time window before movement onset; because in this control task the mean RT was about 310 ms (SD=30 ms), delivering TMS 160 or 200

ms after the target display was necessary to investigate the same time window with respect to the movement onset. Eight blocks of 84 trials were performed in which the 3 TMS conditions (no TMS, TMS at 160 ms and TMS at 200 ms), the 7 shifts of the second target (-6, -4, -2, 0, 2, 4, 6 deg) and the 2 hemifields (left and right) were tested randomly 16 times each. In addition, 2 blocks of 40 trials (exact same conditions as in Experiment #1), were performed to replicate the effect of TMS on the initial movement direction.

Experiment #4. This third control experiment was designed to investigate whether the increased variability in the initial movement direction (DIR_{VE}, see Results of Experiment #1) resulted from an inaccurate outcome of the sensorimotor transformation. To do so, we compared two experimental conditions in which the variability in the initial movement direction was increased by the same amount, with respect to the control condition, but by using two different procedures: 1) DIR_{VE} was increased, as in Experiment #1, by applying TMS over mIPS, 2) it was increased by slightly varying the target direction, in the absence of TMS. Importantly in these two experimental conditions, the mean initial direction was identical. The aim of this experiment was to determine whether these two identical DIR_{VE} values would, irrespective of their origins, lead to the same muscle recruitment pattern. If so, this could be regarded as evidence that the changes in the muscle recruitment pattern reported in Experiment #1 resulted from an adequate adjustment to an inaccurate target localization. In contrast, if two comparable DIR_{VE} values led to two different muscle recruitment patterns, this would indicate that the change in muscle recruitment pattern consequent to mIPS virtual lesions resulted from a corrupted outcome of the sensorimotor transformations leading to the increase in DIR_{VE} reported in Experiment #1.

This experiment was performed in 6 subjects (who participated in Experiment #1; mean age: 27.3±6.7 years). In this experiment, a first block of 40 trials was performed to measure the mean movement onset time for each individual. Next, 2 blocks of 40 trials each were performed in order to corroborate the effects found in Experiment #1. TMS was applied over the left mIPS, on average, 130 ms before movement onset, a timing at which TMS has been shown to affect the initial movement direction (DIR) of visually-guided movements (see Results of Experiment #1). Then, for each trial of each subject, we computed the deviation in DIR induced by TMS when applied over left mIPS. Finally, in two additional blocks (40 trials each), performed without TMS, the targets 1 and 2 (see Fig. 1) were displayed at the same eccentricity (7 deg.) as in Experiment #1 but at locations matching exactly the individual DIR deviation induced by TMS for these 2 targets and measured in the two previous TMS blocks. The two other targets (3 and 4) were presented at the same position as in Experiment #1; in these 2 blocks, all four targets were randomly presented. TMS was only applied over the left mIPS to minimize the number of conditions.

Data acquisition and analysis

The position of the manipulandum was computed from the output signals of two potentiometers (sampling rate: 1 kHz; PCI-6023E, National Instruments, Austin, TX) stored on a personal computer for offline analysis. Then, these signals were low-pass filtered offline (16 Hz) with a fourth order, zero-phase-lag, Butterworth filter (see (Davare et al. 2007a) for details). Electromyographic (EMG) activity was recorded from four right forearm muscles: *extensor carpi radialis longus* (ECRL), *extensor carpi ulnaris* (ECU), *flexor carpi*

radialis (FCR) and *flexor carpi ulnaris* (FCU, Fig. 1C). These four muscles were selected because their pulling direction was nearly identical to the direction of the movements required to reach each target (Hoffman and Strick 1999). The ECRL, ECU, FCU and FCR were acting as agonists for movement performed towards targets #1, #2, #3 and #4, respectively and as antagonists for the opposite targets; they acted as stabilizers when their pulling direction was orthogonal to the target direction. EMG signals were recorded from surface electrodes (Neuroline, Medicotest, Denmark) placed 20 mm apart. The raw EMG signal was amplified (gain: 1K), digitized at 1 kHz and stored on a personal computer for offline analysis. EMG signals were then rectified and low-pass filtered with a fourth order zero-phase-lag Butterworth filter (16 Hz). For each muscle, the presence of an EMG burst was detected automatically in individual trials provided the EMG signal exceeded, for at least 10 successive samples, 25% of the maximal EMG amplitude found in that trial; the peak value of the burst and its time of occurrence with respect to the movement onset were then measured (Hoffman and Strick 1999).

The following parameters were also computed: (1) the reaction time (RT) defined as the delay between target onset and movement onset, (2) the movement time (MT), defined as the delay between the wrist movement onset (the time when the wrist position exceeded the baseline +2 SD) and the entrance of the cursor into the target, provided it remained inside the target for at least 700 ms. (3) The displacement ratio (DR), measured by computing the ratio between the total distance travelled by the wrist to reach the target and the shortest distance between the screen centre and target. DR provided a reliable estimate of the movement trajectory length, a unitary DR value corresponding to a straight wrist displacement from the screen centre to the target (Davare et al. 2007a). (4) The velocity and

acceleration peaks, considered as immune from feedback corrections because of their very short latencies (55.8±10.2 and 25.2±8.5 ms after movement onset, respectively) were used to infer indirectly the planned movement amplitude (Prablanc and Martin 1992; Desmurget et al. 2005). (5) The initial movement direction (DIR), measured by computing the direction of the velocity vector at the acceleration peak, was used to determine the initial movement direction, before any feedback may occur (Prablanc and Martin 1992; Desmurget *et al.* 2005). (6) The constant (DIR_{CE}) and variable errors (DIR_{VE}) of initial movement direction, which measure, respectively, the deviation from the target direction and the inconsistency, or variability, of the movement direction (Schmidt 1976). These measures are important because TMS could not only induce a systematic bias in the movement direction (DIR_{CE}) but also influence its variability (DIR_{VE}).

Firstly, we analysed the effect of TMS applied over the left or right mIPS 100 or 200 ms after target presentation. Delivering TMS at 100 or 200 ms after target presentation had no effect on the reaction time (all $F<1$). Regarding the other movement parameters (MT, DR, DIR_{VE}), there was only a trend towards an effect of TMS delivered at 100 ms. This can be explained by the fact that TMS effects only occur in a very narrow time window. By taking the original TMS 100 ms timing, one would average trials falling in the effective time window with trials falling outside, thus decreasing the magnitude of the observed TMS effects. Therefore, in order to determine more precisely the time course of the effects of mIPS virtual lesions on these different movement parameters, each trial was categorized according to the actual delay between TMS pulse and movement onset and assigned to one of the twelve bins (bin width: 20 ms) spanning over 240 ms, from 200 ms before and 40 ms

after movement onset. For each subject and for each bin, an average value of the different movement parameters was computed, provided that at least 3 data points were available in that bin; mean values were then averaged for all subjects (Davare et al. 2007a).

In Experiment #3, subjects' responses were recorded and stored using Matlab software (Mathworks, Natick, MA). The percentage of 'right arrow key' responses was plotted against the angular distance between the first and second target, and was fitted with a logistic function for each subject and each condition:

$$P_R = 1/(1+exp(\beta 0+\beta 1x)),$$

in which P_R is the probability of 'right' response, x is the offset between the first and second targets, in degrees, and $\beta 0$ and $\beta 1$ are the parameters. The threshold, or point of subjective equality, of this function is defined as the point on the X-axis for which the first derivative of the function is maximal (inflexion point), and the slope of the function corresponds to the value of the first derivative at this point.

Statistical analysis

Because parameters of control movements gathered under the sham condition were not statistically different across blocks (ANOVA, all $F<1$), these data were pooled together and used as a baseline in the following statistical analyses. Repeated measure ANOVA ($ANOVA_{RM}$) were performed with TMS (TMS over left mIPS, TMS over right mIPS or sham), DELAY (12 bins) and TARGET POSITION (left or right hemifield) as within-subject factors. In Experiment #2, $ANOVA_{RM}$ were performed on the velocity and acceleration peaks with TARGET ECCENTRICITY as an additional factor (10, 15 or 20 deg). In Experiment #3, $ANOVA_{RM}$ were performed on both the slope and threshold of the fitted logistic functions, with TMS and

TARGET POSITION as within-subject factors. In Experiment #4, $ANOVA_{RM}$ were used to compare the effects of left mIPS virtual lesions and of "noise" addition in the target location on the muscle recruitment pattern (timing and peak EMG amplitude) for both for clockwise and anticlockwise movement deviations. For all experiments, planned post-hoc comparisons (each bin with respect to the baseline control value) were performed using Dunnett's test (Winer 1971).

Results

Effects of mIPS virtual lesions on visually-guided movements

In Experiment #1, we found that virtual lesions of mIPS impaired movement kinematics as shown by an increased movement trajectory (DR), a longer movement duration (MT) and a larger variable error in the initial movement direction (DIR_{VE}) ($ANOVA_{RM}$: TMS×DELAY×TARGET POSITION, all $F>5.32$, all $p<0.027$); the other movement parameters were unaffected by mIPS virtual lesions (Table 2). Post-hoc analyses showed that TMS led to an increase in DR, MT and DIR_{VE} only for certain delays and only for movements directed toward targets in the contralateral hemifield. Indeed, virtual lesions of left mIPS yielded an increase in DR, MT and DIR_{VE} for movements performed towards the right targets and only when TMS was applied 100-160 ms before movement onset (all $t>3.28$, all $p<0.012$, Fig. 2A and 2B); TMS had no effect when delivered outside this time window (all $t<1.47$, all $p>0.05$; Table 2) and when movements were performed towards left targets (all $t<1.58$, all $p>0.05$). Identical

results were obtained after right mIPS TMS: DR, MT and DIR_{VE} were significantly increased when compared to controls only for movements directed toward the left targets and when lesions were performed 100-160 ms before movement onset (all $t>5.32$, all $p<0.008$). Because DIR_{VE} was found highly correlated with DR ($R=0.84$, $p<0.001$), this suggests a possible causal relationship between these two effects. In addition, it is worth mentioning that, although virtual mIPS lesions systematically yielded a larger DIR_{VE}, it never affected DIR_{CE} (both $F<1$). Indeed, as illustrated in Figure 3B and 3C, DIR_{VE} clearly increased for movements performed towards contralateral targets whereas DIR_{CE} remained undistinguishable from controls (Fig. 3A). In addition, a virtual lesion of either the left or right mIPS led to similar deficits in movements performed toward contralateral targets (post-hoc: all $p>0.05$, see Fig. 3). Finally, it is noteworthy that mIPS lesions never affected the acceleration peak, nor its variability (SD) (Table 2, all $F<1$), a finding of particular importance because the acceleration peak reveals the movement amplitude planned by the subject before any visual feedback is available (Desmurget *et al.* 2005).

To investigate further this absence of effect of mIPS virtual lesions on movement amplitude, in a first control experiment (Experiment #2) the four targets were presented, at random, at 3 different eccentricities (see Methods). As already shown by Hoffman and Strick (1999), we confirmed that the velocity peak increased linearly with the target eccentricity (linear regression: slope=1.38±0.23, mean±SD, n=6; Fig. 4), and therefore with movement amplitude. Similar results were found for the acceleration peak (linear regression: slope=2.07±0.39, mean±SD, n=6). In line with these results, we found a significant main effect of TARGET ECCENTRICITY on velocity and acceleration peaks ($ANOVA_{RM}$ TARGET ECCENTRICITY, both $F>4.93$, both $p<0.011$). Importantly, neither the velocity peak nor the acceleration

peak was altered by TMS applied over the left or right mIPS ($ANOVA_{RM}$ main effect of TMS and TMS× TARGET ECCENTRICITY, all $F<1$).

Effects of mIPS virtual lesions on muscle recruitment

As mentioned in the Introduction, one advantage of this step-tracking task is that it allows us to quantify in great details the pattern and time course of muscle activity accompanying the wrist movements (Hoffman and Strick 1999). In the control condition of Experiment #1, the peak activity in the muscles acting as agonist occurred 6.3±7.6 ms after the actual movement onset (mean of all 4 muscles for all 9 subjects). The activity of muscles, when they acted as antagonist, peaked at 66.3±12.7 ms after wrist movement onset (Fig. 5A). The two other muscles, whose pulling direction is orthogonal to that of the movement, are named "stabilizers" because they contribute to fine-tune and to steady the movement direction. Indeed, both their recruitment order and contraction level permit to adjust the movement curvature (Hoffman and Strick 1999). In the present study, the peak activity of both stabilizers occurred, on average, 34.7±13.2 ms after movement onset in the control conditions. The peak latencies of the agonist, antagonist and stabilizers found in the present study are consistent with those reported by Hoffman and Strick (1999).

We found that mIPS virtual lesions only altered the time course of the stabilizer contraction, the recruitment of the agonist and antagonist being unaffected. Indeed, TMS led to a significant increase in the variability of the stabilizer peak latencies ($ANOVA_{RM}$ on the SD, TMS×DELAY×TARGET, both $F>7.03$, both $p<0.023$, Fig. 5B and 5C) whereas the mean value of these latencies was preserved ($ANOVA_{RM}$, both $F<1$). As described above for DR, MT and

DIR_{VE}, the TMS-induced changes in stabilizer recruitment were only observed when virtual mIPS lesions were induced i) 100 to 160 ms before movement onset and ii) during the preparation of movements directed towards contralesional targets (post-hoc analyses all $t>4.37$, all $p<0.005$, Fig. 2C, Table 2). This congruence indicates a possible causal link between the abnormal timing of stabilizer contraction and the deficits observed in movement kinematics.

To examine further the consequences of mIPS lesions on the stabilizer recruitment, trials were categorized according to the direction - clockwise or anticlockwise - of the TMS-induced deviation of visually-directed movements (Fig. 5B and 5C). Then, for these two groups of trials, we analysed separately, for each individual trial, the activity of the stabilizers whose pulling direction was either clockwise or anticlockwise. In trials in which TMS induced a clockwise deviation of reaching movements, the peak of the "clockwise stabilizer" was much more dispersed in time than that of the "anticlockwise stabilizer" (both $F>6.35$, both $p<0.026$, Fig. 5B). In addition, although the amplitude of the "clockwise stabilizer" was normal, the "anticlockwise stabilizer" had a lower peak amplitude than the clockwise stabilizer (both $F>5.63$, both $p<0.018$, Fig. 5B). Comparable results were found for trials in which TMS induced an anticlockwise deviation (Fig. 5C). Therefore, one possible explanation for the deficits in movement direction consequent to mIPS lesions is an unbalanced contraction of the two stabilizers, due to an inexact outcome of the sensorimotor transformations. Alternatively, it cannot be ruled out that this abnormal recruitment pattern of stabilizers unveiled the consequences of TMS-induced error in computing the correct target position, a necessary condition to plan appropriate reaching movements. We addressed these issues in the next two control experiments.

Effect of mIPS lesions on target localisation

In order to investigate whether the DIR_{VE} increase reported in Experiment #1 could be explained by a deficit in processing the target location, we ran a match-to-sample control experiment (Experiment #3) in which participants had to discriminate the difference between the positions of two visual stimuli displayed sequentially; these stimuli had the same size and eccentricity as the targets used in the step-tracking task. The outcome variable was the probability to report that the second visual target was shifted clockwise with respect to the first one (Fig. 6); these values were plotted as a function of the angular distance between the two stimuli and then fitted with a logistic function (mean $R=0.996\pm0.005$, $n=8$), from which two parameters were computed: 1) the slope, which can be regarded as an estimate of the variable error in discriminating the two stimuli 2) the threshold, which represents the constant error, or the point of subjective equality. We found that neither the slope nor the threshold were affected by the TMS condition ($ANOVA_{RM}$: main effect of TMS: slope: $F=0.24$, $p=0.79$, threshold: $F=1.30$, $p=0.30$; interaction TMS x TARGET POSITION: slope: $F=1.54$, $p=0.25$, threshold: $F=0.61$, $p=0.56$). We only found a significant effect of TARGET POSITION (left versus right hemifield) on the threshold ($F=20.22$, $p=0.003$). This effect consisted in a higher probability to report the second target as located to the left (anti-clockwise rotation) of the first one when displayed in the left hemifield, and to the right (clockwise rotation) when presented in the right hemifield (Fig. 6). Finally, in the 2 blocks in which subjects performed visually-guided movements, we replicated exactly the results of the main experiment i.e. TMS over left mIPS yielded a larger DR, MT and DIR_{VE}

($ANOVA_{RM}$: TMS×DELAY×TARGET POSITION, all $F>4.38$, all $p<0.031$), further corroborating the results of Experiment #1.

Role of mIPS in implementing the direction vector of visually-guided movements

This last control experiment was designed to determine whether the increased scattering in movement direction found in Experiment #1 could be explained by an inexact outcome of the sensorimotor transformations resulting from mIPS virtual lesions. In Experiment #4, 2 out of the 4 targets used in Experiment #1 (targets 1 and 2, see Fig. 1B) were displayed at the same eccentricity but in a slightly different direction in order to mimic the increased DIR_{VE} induced by mIPS virtual lesions in previous experiments. To do so, the different target positions required to obtain comparable DIR_{VE} were exactly calculated for each subject from data gathered at the beginning of each experiment, in 2 TMS blocks in which TMS was applied over left mIPS; DIR was measured for each individual trial and then added to the target position to reproduce the same DIR_{VE} in absence of TMS, by shifting the target position (see Methods). This approach allowed us to compare the recruitment pattern of the stabilizers in two distinct conditions: one in which DIR_{VE} increased following mIPS lesions (Fig. 7B) and another condition, without TMS, in which DIR_{VE} increased because of a "noisy" target location (Fig. 7C). Assuming that the same DIR_{VE} values should lead to the same stabilizer recruitment pattern, we predicted that, if the TMS-induced increase in DIR_{VE} found in Experiment #1 resulted from an inaccurate outcome of the sensorimotor transformations, an increased DIR_{VE} induced by a "noisy" target location should lead to a distinct stabilizer recruitment pattern. In contrast, if injecting some "noise" in the target position replicates the stabilizers' recruitment pattern induced by mIPS virtual lesions, this

would suggest that mIPS virtual lesions altered the target localisation processing per se and that this is a likely explanation for the noisy stabilizer recruitment pattern reported in Experiment #1. The results of this control experiment support the former hypothesis.

Importantly, this control experiment allowed us to confirm again the results of Experiment #1: TMS delivered over left mIPS 130 ms before movement onset led to an increase in DIR_{VE}, MT and DR only for the contralateral targets ($ANOVA_{RM}$, all $F>4.32$, all $p<0.031$; Fig. 8B and C). Moreover, as shown in Figure 7, injecting some "noise" in the position of targets 1 and 2 (right targets) led to a DIR_{VE} identical to that induced by left mIPS lesions ($F<1$, Fig. 7B and C), confirming the effectiveness of our task manipulation. In the "noisy target location" condition, we found that, when the target was shifted "clockwise", the contraction of the "clockwise stabiliser" occurred earlier and was larger ($ANOVA_{RM}$: clockwise stabiliser peak latency and amplitude; both $F>5.23$, both $p<0.017$) than in the control trials (non-shifted targets 3 and 4); the recruitment pattern of the "anticlockwise stabiliser" was unchanged (Fig. 8D). Critically, such an earlier and stronger contraction of the "clockwise stabilizer" was never observed in visually-directed movements deviated clockwise following an mIPS virtual lesion ($ANOVA_{RM}$ on peak latency and amplitude of stabilizers in mIPS TMS vs "noisy target location" conditions: both $F>4.58$, both $p<0.013$; compare Fig. 8B and D). Comparable results were found when the target was shifted anticlockwise (all $F>5.78$, all $p<0.022$, Fig. 8C and E).

Discussion

The present study demonstrates that mIPS is distinctively involved in implementing the direction vector of visually-guided movements performed towards contralateral targets. We found that the main consequence of mIPS "virtual lesions" occurring during the preparation of goal-directed movements was an increased scattering in the initial direction of movements towards contralateral targets, leading to on-line path corrections and, therefore, increased trajectories and longer movement durations. We also found that mIPS lesions induced a change in the recruitment pattern of the stabilizer muscles, which fine-tune the movement direction; this change is likely to be at the origin of the increased variability in the initial movement direction. This conclusion is further supported by the results of a control experiment showing that mIPS virtual lesions did not alter the target localization. We also provided evidence that mIPS virtual lesions did not affect the amplitude of reaching movements. Finally, the present study failed to reveal any hemispheric dominance in programming the direction of visually-guided movements since lesions of either mIPS symmetrically affected movements performed towards contralateral targets.

Before discussing further these results, it is critical to rule out that the effects reported in the present study may have resulted from non-specific TMS effects. Importantly, the parameters found to be affected by virtual lesions of mIPS were complex movement parameters (DIR_{VE}, DR and MT), unlikely, as the reaction time, to be influenced by the TMS noise or tactile scalp stimulation; this conclusion is further strengthened by an absence of effects in the sham TMS condition. In addition, these movement parameters were only affected when TMS was applied during a very narrow time window (100-160 ms before

movement onset) and for movements planned towards contralateral targets. Finally, we have recently reported that, in subjects performing the same step-tracking task, TMS applied over the primary motor (M1) or the dorsal premotor cortex affects distinct movement parameters at different timings (Davare et al. 2007a; Davare et al. 2007b). Altogether, these different arguments support the specificity of the effects described in the present study.

The present study corroborates the conclusions of several neuroimaging studies showing that mIPS - regarded as the homologue of the medial intraparietal area (MIP) originally described in monkeys (Colby et al. 1988; Johnson et al. 1996; Eskandar and Assad 1999, 2002; Grefkes and Fink 2005; Archambault et al. 2009) - is critically involved in controlling reaching movements in humans (Astafiev *et al.* 2003; Connolly *et al.* 2003; Medendorp *et al.* 2005; Prado *et al.* 2005; Culham *et al.* 2006; Culham and Valyear 2006; Blangero *et al.* 2009; Hinkley *et al.* 2009). Although most of these functional imaging studies have reached a consensus about the involvement of mIPS in visually-guided hand movements, earlier attempts made to determine the causal role of this area remained inconclusive, likely because previous TMS studies have used a variety of motor tasks and have potentially targeted different PPC areas (see Introduction). In the present study, we carefully controlled the stimulation sites and used a simple well-defined motor task (Hoffman and Strick 1999) and found that mIPS lesions altered the recruitment pattern of the stabilizer muscles, suggesting that mIPS determines the direction of reaching movements. The view that mIPS is involved in coding the movement direction in motor coordinates is consistent with the study of Vesia et al. (2006) showing that a single pulse

TMS applied over the right dorso-lateral PPC systematically yielded a leftward pointing bias which persists when subjects wore optical reversing prisms. In addition, in another recent study, Vesia and collaborators reported that the amount of visual information about the hand position available during the initial phase of reaching movements changed the effects of dorso-lateral PPC virtual lesions. Indeed, reaching errors induced by TMS decreased when the initial hand position could be used to define the reach vector, further suggesting that motor-related information, rather than the visual goal, is processed by mIPS (Vesia *et al.* 2008). Our conclusion that mIPS is critically involved in the implementation of the motor vector subserving visually-guided movements is also compatible with the results of a recent functional imaging study showing that, during pointing movements, mIPS is activated bilaterally and irrespective of the gaze position (Prado *et al.* 2005). This clearly suggests an involvement of mIPS at a later stage of the sensorimotor transformation, closer to the motor output than to the sensory processing stage.

Importantly, the present study also demonstrates that the deficits in visually-guided movements induced by mIPS virtual lesions cannot be explained in terms of errors in processing the target location. Indeed, a match-to-sample control experiment failed to reveal any effect of mIPS virtual lesions on the capacity to discriminate the target location, at least inside the time window investigated in Experiment #3. In addition, we found that introducing some noise in the target location – in order to mimic a possible effect of TMS – did no yield the same pattern of muscle activity as that observed following mIPS lesions (Experiment #4). Altogether, these findings suggest that mIPS is not involved in processing the target location, and further corroborate our conclusion that mIPS contributes to a later

stage of the sensorimotor transformations underlying visually-guided movements, However, this claim may appear at odds with respect to monkey studies showing that MIP also encodes target location (Johnson *et al.* 1996). It is possible that the deepest part of mIPS, which in monkey is known to contain neurons showing a target-related activity, was not accessible by TMS, hence only disrupting the most superficial part of mIPS that could be selectively involved in processing movement direction (Johnson et al. 1996). Alternatively, it cannot be ruled out that we failed to evidence the contribution of mIPS to the target position processing because it occurs earlier during movement preparation. However, our conclusion that mIPS is not involved in processing the target position is congruent with the results of several functional imaging studies showing that processing the target position may occur in more posterior occipito-parietal areas (Prado *et al.* 2005; Beurze *et al.* 2009; Blangero *et al.* 2009; Filimon *et al.* 2009). Apart from these points, it is also worth mentioning that visuo-spatial processing remains difficult to investigate because it is easily confounded with other cognitive functions such as spatial attention (Curtis 2006). Other brain structures commonly associated with visuo-spatial processing are the dorso-lateral prefrontal cortex, the superior parietal lobule and some areas in the intraparietal sulcus such as the lateral (LIP) and ventral (VIP) intraparietal areas. In a TMS study investigating the neural substrate of visuo-spatial processing, Oliveri and collaborators showed that whereas a unilateral stimulation of PPC (P4 or P5) failed to affect performance in a visuo-spatial task, a bilateral stimulation was effective in altering the reaction times (Oliveri et al. 2001). While this study did not attempt to dissociate perceptive from memory processes, and did not clearly identify the targeted area, it suggests that an interaction between left and right parietal cortex is

critical for processing of the localization of visual targets. Another study by Mottaghy et al. (2002) investigated the role of different prefrontal areas in a spatial localization and face recognition tasks by using rTMS (Mottaghy et al. 2002). They found that whereas the disruption of left ventral prefrontal cortex affected only performance in the face recognition task, rTMS applied over the left dorsolateral prefrontal cortex perturbed specifically the localization task. These results, together with functional neuroimaging studies (reviewed in (Curtis 2006), converge to suggest that a complex network involving multiple areas in the PPC is involved in encoding and/or storing visuo-spatial information.

Another interesting result of the present study is that the velocity and acceleration peaks were not modified following mIPS virtual lesions, suggesting that this area is not involved in the early computation, or the implementation, of movement amplitude (Desmurget *et al.* 2005). Interestingly, the deficits in movements we found following mIPS virtual lesions are reminiscent of observations made in patients with optic ataxia, who mainly present an increased directional errors with no biases in movement amplitude (Perenin and Vighetto 1988; Darling et al. 2001; Karnath and Perenin 2005). Such a dissociation between the direction and amplitude of goal directed movements is also consistent with a large body of literature suggesting that the basal ganglia (Desmurget et al. 2004; Krakauer et al. 2004; Desmurget and Turner 2008) are involved in planning the amplitude of reaching movements, likely in hand-centred coordinates (Gordon et al. 1994; Vindras et al. 2005). As emphasized in a recent study (Ferraina et al. 2009) such a dissociation seems to support the idea that reaching movements are planned through a cascade of sensorimotor transformations from a retinotopic to a binocular viewer-centred to a hand-centred reference frame (for a comprehensive discussion (Burnod et al. 1999;

Battaglia-Mayer et al. 2003). Finally, it is worth mentioning a recent TMS study investigating the functional specificity of different subregions in the PPC during saccade and reaching tasks (Vesia et al. 2010). These authors reported different effector-specific parietal regions that could underlie this cascade of sensorimotor transformations occurring in distinct reference frames during preparation of visually guided movements (Vesia et al. 2010). Whereas SPOC encodes retinally peripheral reach goals, more anterior-lateral regions (mIPS and the angular gyrus) along the IPS possess overlapping maps for saccade and reach planning and are more closely involved in motor implementation. Although in the present study we only interfered with the function of a given area within the PPC, our results are in close agreement with the conclusion of Vesia and collaborators.

Finally, the question arises as to whether our findings can be generalised to whole-arm reach-to-grasp movements. Three lines of evidence support this viewpoint. First, it has been shown that the execution of wrist step-tracking movements activate the same parietal areas as reaching movements (Grefkes et al. 2004). Secondly, the step-tracking task used in the present study relies inevitably on the computation of the same movement parameters as whole-arm reach-to-grasp movements, namely the direction and amplitude (Gordon et al. 1994; Vindras et al. 2005). These two parameters define a motor vector that will be subsequently transformed into a motor command sent to wrist muscles (in the step-tracking task) or distributed to more proximal arm muscles (in a whole-arm reaching task), taking into account different degrees of freedom (d'Avella et al. 2006). Finally, using a whole-arm reaching task, Vesia et al. (2010) have recently shown that TMS over mIPS

increased the endpoint movement variability when vision of the moving hand is prevented, a finding in agreement with the increase in initial movement direction variability in our study in which continuous visual-feedback allowed the subjects to correct this increased initial variability on-line. Therefore, it is sensible to assume that our findings can be generalized to whole-arm reach-to-grasp movements and we predict that mIPS virtual lesions would likewise alter the direction of reach-to-grasp movements, by resulting in a inaccurate computation of the motor vector required to transport the hand towards the object to be grasped. Our results complement the findings of Vesia et al. (2010) by showing that mIPS encodes a direction motor vector regardless of whether it underlies a arm movement or a wrist rotation. Furthermore, because the PPC contains distinct functional modules for controlling the arm transport and grip components of reach-to-grasp movements (Cavina-Pratesi et al. 2010; Davare et al. 2010; Davare et al. 2011), we predict that mIPS virtual lesions would leave the grip component unaffected.

Acknowledgements

This work was supported by grants from the "Actions de recherches concertées“ (ARC, Académie Louvain), the Fonds Spéciaux de Recherche” (FSR) of the Université catholique de Louvain, the “Fonds de la Recherche Scientifique Médicale” (FRSM) and the “Fondation Médicale Reine Elisabeth” (FMRE).

The authors are grateful to P.L. Strick for his help with the manipulandum design and also to M. Penta for his help with data acquisition.

References

Archambault PS, Caminiti R, Battaglia-Mayer A. 2009. Cortical mechanisms for online control of hand movement trajectory: the role of the posterior parietal cortex. Cereb Cortex. 19: 2848-2864.

Astafiev SV, Shulman GL, Stanley CM, Snyder AZ, Van Essen DC, Corbetta M. 2003. Functional organization of human intraparietal and frontal cortex for attending, looking, and pointing. J Neurosci. 23: 4689-4699.

Battaglia-Mayer A, Caminiti R, Lacquaniti F, Zago M. 2003. Multiple levels of representation of reaching in the parieto-frontal network. Cereb Cortex. 13: 1009-1022.

Beurze SM, de Lange FP, Toni I, Medendorp WP. 2009. Spatial and effector processing in the human parietofrontal network for reaches and saccades. J Neurophysiol. 101: 3053-3062.

Blangero A, Menz MM, McNamara A, Binkofski F. 2009. Parietal modules for reaching. Neuropsychologia. 47: 1500-1507.

Burnod Y, Baraduc P, Battaglia-Mayer A, Guigon E, Koechlin E, Ferraina S, Lacquaniti F, Caminiti R. 1999. Parieto-frontal coding of reaching: an integrated framework. Exp Brain Res. 129: 325-346.

Cavina-Pratesi C, Monaco S, Fattori P, Galletti C, McAdam TD, Quinlan DJ, Goodale MA, Culham JC. 2010. Functional magnetic resonance imaging reveals the neural substrates of arm transport and grip formation in reach-to-grasp actions in humans. J Neurosci. 30: 10306-10323.

Colby CL, Gattass R, Olson CR, Gross CG. 1988. Topographical organization of cortical afferents to extrastriate visual area PO in the macaque: a dual tracer study. J Comp Neurol. 269: 392-413.

Connolly JD, Andersen RA, Goodale MA. 2003. FMRI evidence for a 'parietal reach region' in the human brain. Exp Brain Res. 153: 140-145.

Culham JC, Cavina-Pratesi C, Singhal A. 2006. The role of parietal cortex in visuomotor control: what have we learned from neuroimaging? Neuropsychologia. 44: 2668-2684.

Culham JC, Valyear KF. 2006. Human parietal cortex in action. Curr Opin Neurobiol. 16: 205-212.

Curtis CE. 2006. Prefrontal and parietal contributions to spatial working memory. Neuroscience. 139: 173-180.

d'Avella A, Portone A, Fernandez L, Lacquaniti F. 2006. Control of fast-reaching movements by muscle synergy combinations. J Neurosci. 26: 7791-7810.

Darling WG, Rizzo M, Butler AJ. 2001. Disordered sensorimotor transformations for reaching following posterior cortical lesions. Neuropsychologia. 39: 237-254.

Davare M, Andres M, Cosnard G, Thonnard JL, Olivier E. 2006. Dissociating the role of ventral and dorsal premotor cortex in precision grasping. J Neurosci. 26: 2260-2268.

Davare M, Duque J, Vandermeeren Y, Thonnard JL, Olivier E. 2007a. Role of the ipsilateral primary motor cortex in controlling the timing of hand muscle recruitment. Cereb Cortex. 17: 353-362.

Davare M, Kraskov A, Rothwell JC, Lemon RN. 2011. Interactions between areas of the cortical grasping network. Curr Opin Neurobiol.

Davare M, Rothwell JC, Lemon RN. 2010. Causal connectivity between the human anterior intraparietal area and premotor cortex during grasp. Curr Biol. 20: 176-181.

Davare M, Zenon A, Olivier E. 2007b. Double dissociation between the role of the medial intraparietal area (MIP) and dorsal premotor cortex (PMd) in reaching movements. 37th Annual meeting of the Society for Neurosciences, San Diego, California, Nov 3-7
. (281.218/HH282).

Deiber MP, Ibanez V, Sadato N, Hallett M. 1996. Cerebral structures participating in motor preparation in humans: a positron emission tomography study. J Neurophysiol. 75: 233-247.

Desmurget M, Grafton ST, Vindras P, Grea H, Turner RS. 2004. The basal ganglia network mediates the planning of movement amplitude. Eur J Neurosci. 19: 2871-2880.

Desmurget M, Grea H, Grethe JS, Prablanc C, Alexander GE, Grafton ST. 2001. Functional anatomy of nonvisual feedback loops during reaching: a positron emission tomography study. J Neurosci. 21: 2919-2928.

Desmurget M, Turner RS. 2008. Testing basal ganglia motor functions through reversible inactivations in the posterior internal globus pallidus. J Neurophysiol. 99: 1057-1076.

Desmurget M, Turner RS, Prablanc C, Russo GS, Alexander GE, Grafton ST. 2005. Updating target location at the end of an orienting saccade affects the characteristics of simple point-to-point movements. J Exp Psychol Hum Percept Perform. 31: 1510-1536.

Eskandar EN, Assad JA. 1999. Dissociation of visual, motor and predictive signals in parietal cortex during visual guidance. Nat Neurosci. 2: 88-93.

Eskandar EN, Assad JA. 2002. Distinct nature of directional signals among parietal cortical areas during visual guidance. J Neurophysiol. 88: 1777-1790.

Fattori P, Breveglieri R, Marzocchi N, Filippini D, Bosco A, Galletti C. 2009. Hand orientation during reach-to-grasp movements modulates neuronal activity in the medial posterior parietal area V6A. J Neurosci. 29: 1928-1936.

Ferraina S, Battaglia-Mayer A, Genovesio A, Archambault P, Caminiti R. 2009. Parietal encoding of action in depth. Neuropsychologia. 47: 1409-1420.

Filimon F, Nelson JD, Huang RS, Sereno MI. 2009. Multiple parietal reach regions in humans: cortical representations for visual and proprioceptive feedback during on-line reaching. J Neurosci. 29: 2961-2971.

Gordon J, Ghilardi MF, Ghez C. 1994. Accuracy of planar reaching movements. I. Independence of direction and extent variability. Exp Brain Res. 99: 97-111.

Grefkes C, Fink GR. 2005. The functional organization of the intraparietal sulcus in humans and monkeys. J Anat. 207: 3-17.

Grefkes C, Ritzl A, Zilles K, Fink GR. 2004. Human medial intraparietal cortex subserves visuomotor coordinate transformation. Neuroimage. 23: 1494-1506.

Hinkley LB, Krubitzer LA, Padberg J, Disbrow EA. 2009. Visual-manual exploration and posterior parietal cortex in humans. J Neurophysiol. 102: 3433-3446.

Hoffman DS, Strick PL. 1986. Step-tracking movements of the wrist in humans. I. Kinematic analysis. J Neurosci. 6: 3309-3318.

Hoffman DS, Strick PL. 1999. Step-tracking movements of the wrist. IV. Muscle activity associated with movements in different directions. J Neurophysiol. 81: 319-333.

Johnson PB, Ferraina S, Bianchi L, Caminiti R. 1996. Cortical networks for visual reaching: physiological and anatomical organization of frontal and parietal lobe arm regions. Cereb Cortex. 6: 102-119.

Karnath HO, Perenin MT. 2005. Cortical control of visually guided reaching: evidence from patients with optic ataxia. Cereb Cortex. 15: 1561-1569.

Keel JC, Smith MJ, Wassermann EM. 2001. A safety screening questionnaire for transcranial magnetic stimulation. Clin Neurophysiol. 112: 720.

Krakauer JW, Ghilardi MF, Mentis M, Barnes A, Veytsman M, Eidelberg D, Ghez C. 2004. Differential cortical and subcortical activations in learning rotations and gains for reaching: a PET study. J Neurophysiol. 91: 924-933.

Mars RB, Jbabdi S, Sallet J, O'Reilly JX, Croxson PL, Olivier E, Noonan MP, Bergmann C, Mitchell AS, Baxter MG, Behrens TE, Johansen-Berg H, Tomassini V, Miller KL, Rushworth MF. 2011. Diffusion-weighted imaging tractography-based parcellation of the human parietal cortex and comparison with human and macaque resting-state functional connectivity. J Neurosci. 31: 4087-4100.

Medendorp WP, Goltz HC, Crawford JD, Vilis T. 2005. Integration of target and effector information in human posterior parietal cortex for the planning of action. J Neurophysiol. 93: 954-962.

Mottaghy FM, Gangitano M, Sparing R, Krause BJ, Pascual-Leone A. 2002. Segregation of areas related to visual working memory in the prefrontal cortex revealed by rTMS. Cereb Cortex. 12: 369-375.

Noirhomme Q, Ferrant M, Vandermeeren Y, Olivier E, Macq B, Cuisenaire O. 2004. Registration and real-time visualization of transcranial magnetic stimulation with 3-D MR images. IEEE Trans Biomed Eng. 51: 1994-2005.

Oldfield RC. 1971. The assessment and analysis of handedness: the Edinburgh inventory. Neuropsychologia. 9: 97-113.

Oliveri M, Turriziani P, Carlesimo GA, Koch G, Tomaiuolo F, Panella M, Caltagirone C. 2001. Parieto-frontal interactions in visual-object and visual-spatial working memory: evidence from transcranial magnetic stimulation. Cereb Cortex. 11: 606-618.

Perenin MT, Vighetto A. 1988. Optic ataxia: a specific disruption in visuomotor mechanisms. I. Different aspects of the deficit in reaching for objects. Brain. 111 (Pt 3): 643-674.

Prablanc C, Martin O. 1992. Automatic control during hand reaching at undetected two-dimensional target displacements. J Neurophysiol. 67: 455-469.

Prado J, Clavagnier S, Otzenberger H, Scheiber C, Kennedy H, Perenin MT. 2005. Two cortical systems for reaching in central and peripheral vision. Neuron. 48: 849-858.

Schmidt RA. 1976. Control processes in motor skills. Exerc Sport Sci Rev. 4: 229-261.

Smyrnis N, Theleritis C, Evdokimidis I, Muri RM, Karandreas N. 2003. Single-pulse transcranial magnetic stimulation of parietal and prefrontal areas in a memory delay arm pointing task. J Neurophysiol. 89: 3344-3350.

Striemer CL, Chouinard PA, Goodale MA. 2011. Programs for action in superior parietal cortex: A triple-pulse TMS investigation. Neuropsychologia.

Vesia M, Monteon JA, Sergio LE, Crawford JD. 2006. Hemispheric asymmetry in memory-guided pointing during single-pulse transcranial magnetic stimulation of human parietal cortex. J Neurophysiol. 96: 3016-3027.

Vesia M, Prime SL, Yan X, Sergio LE, Crawford JD. 2010. Specificity of human parietal saccade and reach regions during transcranial magnetic stimulation. J Neurosci. 30: 13053-13065.

Vesia M, Yan X, Henriques DY, Sergio LE, Crawford JD. 2008. Tms over Human Dorsal-Lateral Posterior Parietal Cortex Disrupts Integration of Hand Position Signals into the Reach Plan. J Neurophysiol. 100: 2005-2014.

Vindras P, Desmurget M, Viviani P. 2005. Error parsing in visuomotor pointing reveals independent processing of amplitude and direction. J Neurophysiol. 94: 1212-1224.

Winer BJ. 1971. Statistical Principles in Experimental Design. New York: McGraw Hill.

Table 1

MNI coordinates of mIPS reported in studies using different approaches

		mIPS	X	Y	Z
Grefkes et al., 2004	fMRI	left	-28	-50	52
		right	28	-56	50
Prado et al., 2005 *	fMRI	left	-25 ± 5	-54 ± 3	66 ± 3
		right	29 ± 5	-56 ± 3	63 ± 2
Stark and Zohary, 2008 *	fMRI region of interest	left	-22 ± 2	-61 ± 1	56 ± 1
		right	31 ± 4	-59 ± 7	48 ± 4
Blangero et al., 2009 *	fMRI meta-analysis	left	-26	-61	58
		right	18	-65	55
Vesia et al., 2010 *	TMS	left	-22 ± 3	-69 ± 6	42 ± 4
		right	26 ± 3	-66 ± 4	41 ± 3
Mars *et al.* 2011	DTI	right	28	-55	55
Striemer *et al.* 2011 *	TMS	left	-30 ± 5	-54 ± 5	49 ± 4
Present study	**TMS**	**left**	**-32 ± 5**	**-49 ± 6**	**46 ± 9**
		right	**33 ± 5**	**-46 ± 7**	**49 ± 10**

Coordinates have been converted into MNI space when originally provided in Talairach space (as indicated by *). Standard deviations are shown when available. Coordinates shown for Prado et al., 2005 are the average of three cluster peaks found in mIPS. fMRI: functional magnetic resonance imaging; TMS: transcranial magnetic stimulation; DTI: diffusion tensor imaging.

Table 2

Effects of mIPS virtual lesions on the step-tracking movement parameters.

	Control	*left mIPS$_{100-160}$*	*p*	*right mIPS$_{100-}$*	*p*
RT [ms]					
Target 1 (45 deg)	214.4 ± 23.2	227.2 ± 19.3	>0.05	217.3 ± 18.5	>0.05
Target 2 (315 deg)	223.3 ± 27.3	234.4 ± 22.7	>0.05	213.6 ± 19.4	>0.05
Target 3 (225 deg)	231.9 ± 24.9	227.5 ± 20.6	>0.05	234.2 ± 21.7	>0.05
Target 4 (135 deg)	219.8 ± 26.4	221.7 ± 19.8	>0.05	229.4 ± 24.9	>0.05
MT [ms]					
Target 1 (45 deg)	380.5 ± 50.4	**457.6 ± 60.2**	**0.002**	374.7 ± 76.1	>0.05
Target 2 (315 deg)	395.4 ± 71.2	**464.8 ± 72.4**	**0.019**	402.7 ± 82.3	>0.05
Target 3 (225 deg)	405.3 ± 65.3	395.4 ± 54.8	>0.05	**487.3 ± 78.3**	**0.017**
Target 4 (135 deg)	377.1 ± 64.2	410.4 ± 76.4	>0.05	**510.3 ± 56.3**	**0.004**
DR					
Target 1 (45 deg)	2.02 ± 0.51	**2.42 ± 0.28**	**0.001**	1.87 ± 0.43	>0.05
Target 2 (315 deg)	2.14 ± 0.35	**2.54 ± 0.34**	**<0.001**	2.05 ± 0.50	>0.05
Target 3 (225 deg)	1.98 ± 0.43	2.08 ± 0.35	>0.05	**2.50 ± 0.54**	**<0.001**
Target 4 (135 deg)	2.01 ± 0.54	2.13 ± 0.43	>0.05	**2.65 ± 0.46**	**<0.001**
Accel. peak (x10^3 deg.s^{-2})					
Target 1 (45 deg)	8.19 ±0.11	8.05 ±0.19	>0.05	8.15 ±0.14	>0.05
Target 2 (315 deg)	8.12 ±0.17	8.21 ±0.16	>0.05	8.06 ±0.13	>0.05
Target 3 (225 deg)	8.05 ±0.15	8.20 ±0.13	>0.05	8.09 ±0.17	>0.05
Target 4 (135 deg)	8.20 ±0.15	8.08 ±0.16	>0.05	8.13 ±0.16	>0.05
DIR [deg]					
Target 1 (45 deg)	48.7 ± 6.5	46.2 ± 14.8	>0.05	50.2 ± 6.4	>0.05
Target 2 (315 deg)	316.2 ± 4.8	313.7 ± 11.2	>0.05	315.5 ± 8.6	>0.05
Target 3 (225 deg)	232.5 ± 8.5	229.3 ± 8.5	>0.05	227.1 ± 13.7	>0.05
Target 4 (135 deg)	128.3 ± 7.2	129.4 ± 7.2	>0.05	130.2 ± 11.2	>0.05
DIR$_{VE}$ [deg]					
Target 1 (45 deg)	6.5 ± 5.4	**14.8 ± 5.7**	**0.012**	6.4 ± 4.2	>0.05
Target 2 (315 deg)	4.8 ± 4.6	**11.2 ± 6.1**	**0.003**	8.6 ± 5.4	>0.05
Target 3 (225 deg)	8.5 ± 5.9	8.5 ± 6.2	>0.05	**13.7 ± 6.4**	**<0.001**
Target 4 (135 deg)	7.2 ± 6.1	7.2 ± 5.1	>0.05	**11.2 ± 7.1**	**0.008**
Stabilizer variability [ms]					
Target 1 (45 deg)	10.1 ± 3.4	**21.7 ± 4.3**	**<0.001**	10.2 ± 4.1	>0.05
Target 2 (315 deg)	12.5 ± 2.6	**19.5 ± 4.9**	**0.005**	9.8 ± 3.7	>0.05
Target 3 (225 deg)	9.4 ± 6.3	7.4 ± 3.2	>0.05	**18.7 ± 3.2**	**0.004**
Target 4 (135 deg)	10.7 ± 4.6	9.3 ± 4.1	>0.05	**20.5 ± 4.1**	**<0.001**

Values are mean±SD (n=9, experiment #1). mIPS: medial part of the intraparietal sulcus; TMS: transcranial magnetic stimulation; TMS$_{100-160}$: TMS occurred 100 to 160 ms before movement onset; MT: movement time; DR: displacement ratio; Accel. peak: acceleration peak; DIR: initial movement direction; DIR$_{VE}$: variable error in the initial movement

direction; Stabilizer variability: SD of the mean latency of the peak activity of both stabilizers. Target numbers are the same as in Fig. 1B.

Legends

Figure 1
Experimental setup.

A. Manipulandum used in the experiment. The subjects had to grasp the handle, which was adjusted so that the centre of rotation of the manipulandum and the wrist joint coincided. The wrist was held in a position midway between pronation and supination.

B. Location of visual targets. The 4 targets used in Experiment #1 are shown simultaneously for illustrative purpose only, in order to show their location (target 1, 2, 3 and 4 respectively in the upper right, lower right, lower left and upper left corner). In the actual experimental conditions, only one target was shown at a time. The central square represents the starting point. Four real movement trajectories were superimposed on the target display. The horizontal and vertical axes represent the flexion-extension and the radial-ulnar axes, respectively.

C. Typical recording of the velocity and EMG activity during the step-tracking task. The inset shows the actual trajectory of this trial. Note that the FCU (acting as agonist) is active first and followed by a burst in the FCR and ECU (acting as stabilizers). The ECRL (acting as antagonist) shows a burst later during movement performance.

D. Mean location of the stimulation points over mIPS in both the left and right hemispheres after normalization into the MNI coordinate system (n=23). The ellipse centre is located over the mean MNI coordinates of each stimulation site; the ellipse surface indicates the 95% confidence interval. The intraparietal sulcus is highlighted in blue.

Figure 2
Time course of the effects of left mIPS lesions.

Data were assigned to bins of 20 ms width. X-axis: delay between TMS triggering and movement onset. Figures A, B and C illustrate, respectively, the effect of left mIPS TMS on the DR, DIR_{VE} (variable error in initial movement direction) and the variability of the latency of the stabilizer peak activity (average of both). Dunnett's t-test multiple comparison procedure: * = $p<0.05$. Note that for right mIPS virtual lesions, the effects were similar, but only for left targets.

Figure 3
Effect of virtual mIPS lesions on the initial movement direction (DIR).

Polar plots showing the amplitude and direction of the velocity vector computed at the peak of acceleration. Figures A, B, C represent, respectively, results from control, left mIPS and right mIPS conditions; for these two latter conditions, only results gathered for the -160 to -100 ms interval are illustrated. The four dashed lines represent the actual target directions. The four black dots indicate the mean amplitude and direction of the velocity vector for each target. Each grey sector indicates ± 2 SD of DIR and shows that the variability in initial movement direction was different from the control values. X- and Y-values are expressed in $deg.s^{-1}$.

Figure 4

Lack of effect of virtual mIPS lesions on the planned movement amplitude.

Velocity peak values (Y-axis) are plotted against the 3 target eccentricities (Experiment #2). A. control (sham) movements. B. TMS delivered over the left or right mIPS. Values are the mean of velocity peaks of movements directed to all four target directions.

Figure 5

Effect of virtual mIPS lesions on the pattern of muscle activity.

Upper row: Typical trials are represented for controls (A) and for movements performed following TMS applied over the left mIPS (B) which induced either a clockwise or anticlockwise deviation.

Middle row: Polar plots showing the amplitude and direction of the velocity vector at the peak of acceleration (see Fig. 3). For the TMS condition (B), trials were grouped according to the deviation induced by TMS, either clockwise (red) or anticlockwise (blue).

Bottom row: The mean±SD of the peak latencies of the agonist (Ag), stabilizer (Stab; average of both stabilizers) and antagonist (Ant) activity are represented respectively by the green, grey and purple rectangles below the X-axis. For stabilizers only, the peak activity and its latency are shown separately for the clockwise (red) and the anticlockwise stabilizer (blue). Movement onset corresponds to 0 ms on the X-axis.

Figure 6

Lack of effect of mIPS virtual lesion on target location (Experiment #3)

The probability of 'rightward' responses as a function of the offset between the first and second target was fitted with a logistic function for the left (upper graph) and right hemifield (lowed graph) and TMS condition (no TMS, TMS at 160 ms and TMS at 200 ms). Note that there is no effect of TMS on neither the slope or the threshold of the logistic function.

Figure 7

Distributions of initial direction (DIR) in Experiment #4

Upper row: Schematic illustration of the experimental protocol used in Experiment #4. A: control movements (n=80: targets 3 and 4 of the 2 TMS blocks and of the 2 "noisy target location" blocks). B: TMS applied on the left mIPS 130 ms before movement onset induced a larger DIR_{VE}, as represented by the larger grey sector. C: condition in which we introduced some noise in the target location by displaying the stimuli at the same DIR as induced by TMS applied over mIPS. Targets were actually displayed at a location in between the 2 extreme targets depicted in the figure.

Bottom row: The DIR distributions are shown by steps of 3 deg. for control movements (A), for left mIPS virtual lesions (B) and for the "noisy target location" condition (C).

Figure 8
Comparison of mIPS lesions and of "noisy target location" effects on the pattern of stabilizer recruitment.

Left: typical trials in each condition of Experiment #4. For left mIPS lesions and "noisy target location", trials were separated according to the direction (clockwise or anticlockwise) of the deviation in reaching movements as induced by TMS (B-C) and due to the target shift (D-E).

Right: Mean±SD of the peak latency and peak activity of both the clockwise (red) and anticlockwise (blue) stabilizers. Note the difference between the recruitment pattern of the stabilizers in the left mIPS TMS and in the "noisy target location" conditions. In the TMS condition, the clockwise stabilizer had a larger variability in its latency peak and the anticlockwise stabilizer had a smaller peak amplitude (B-C). In the "noisy target location" condition, the peak of the clockwise stabilizer was higher and occurred earlier than in controls whereas the anticlockwise stabilizer remained unchanged (D-E).

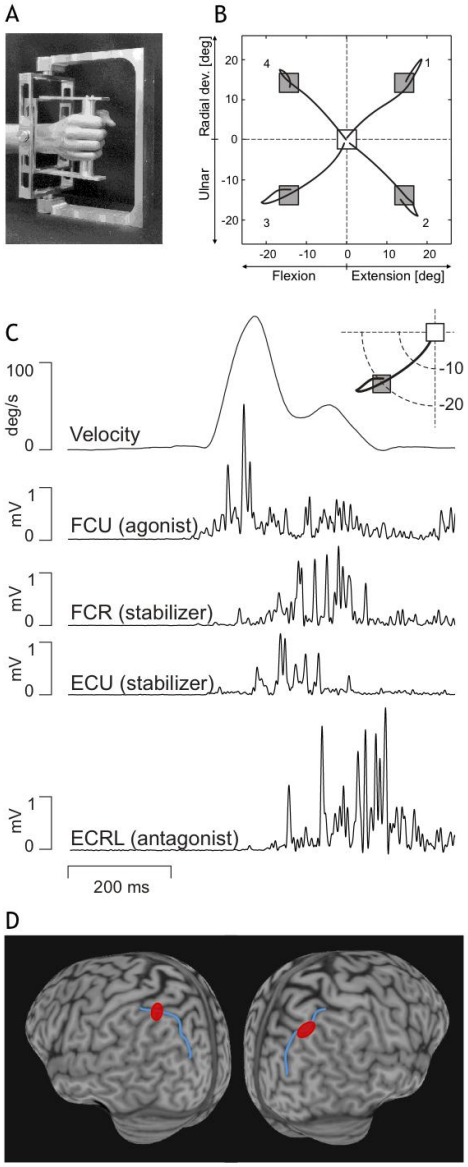

Davare_PPC_Fig. 1

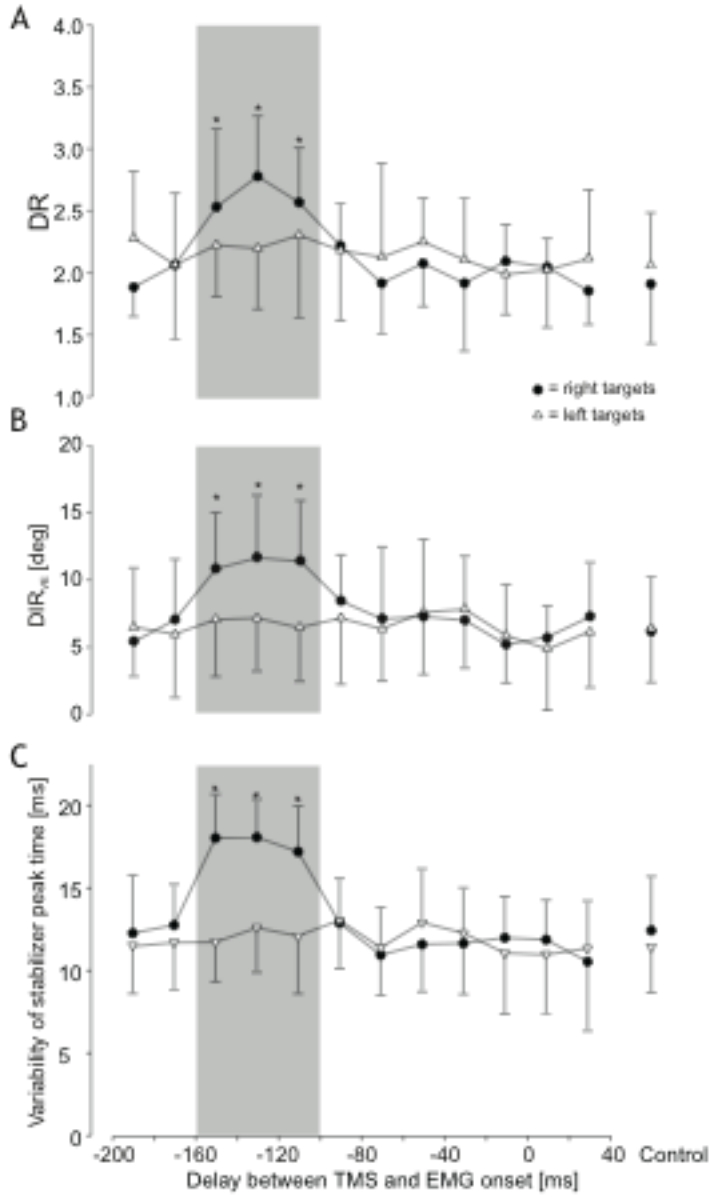
A
DR
4.0
3.5
3.0
2.5
2.0
1.5
1.0
● = right targets
△ = left targets
B
DIR_xc [deg]
20
15
10
5
0
C
Variability of stabilizer peak time [ms]
20
15
10
5
0
-200
-160
-120
-80
-40
0
40
Control
Delay between TMS and EMG onset [ms]

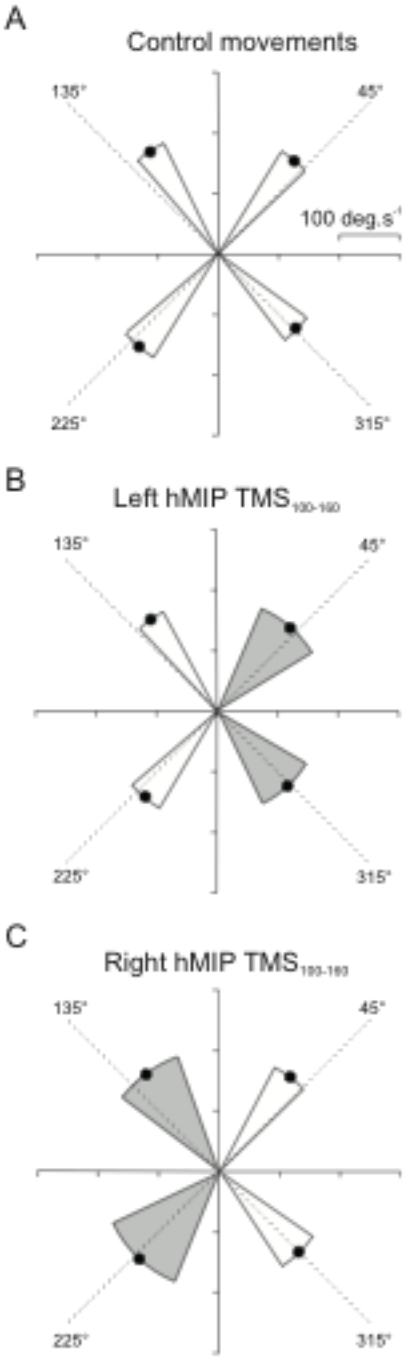
A
Control movements
135°
45°
100 deg.s-1
225°
315°
B
Left hMIP TMS100-160
135°
45°
225°
315°
C
Right hMIP TMS100-160
135°
45°
225°
315°

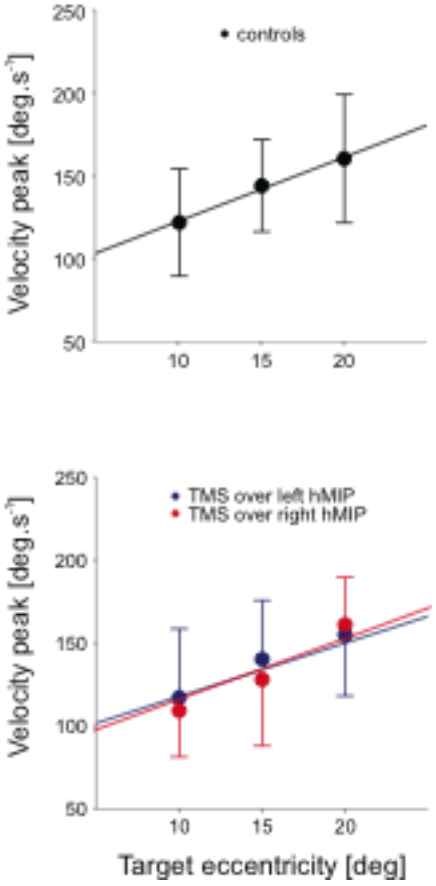
controls
Velocity peak [deg.s-1]
250
200
150
100
50
10
15
20
TMS over left hMIP
TMS over right hMIP
Velocity peak [deg.s-1]
250
200
150
100
50
10
15
20
Target eccentricity [deg]

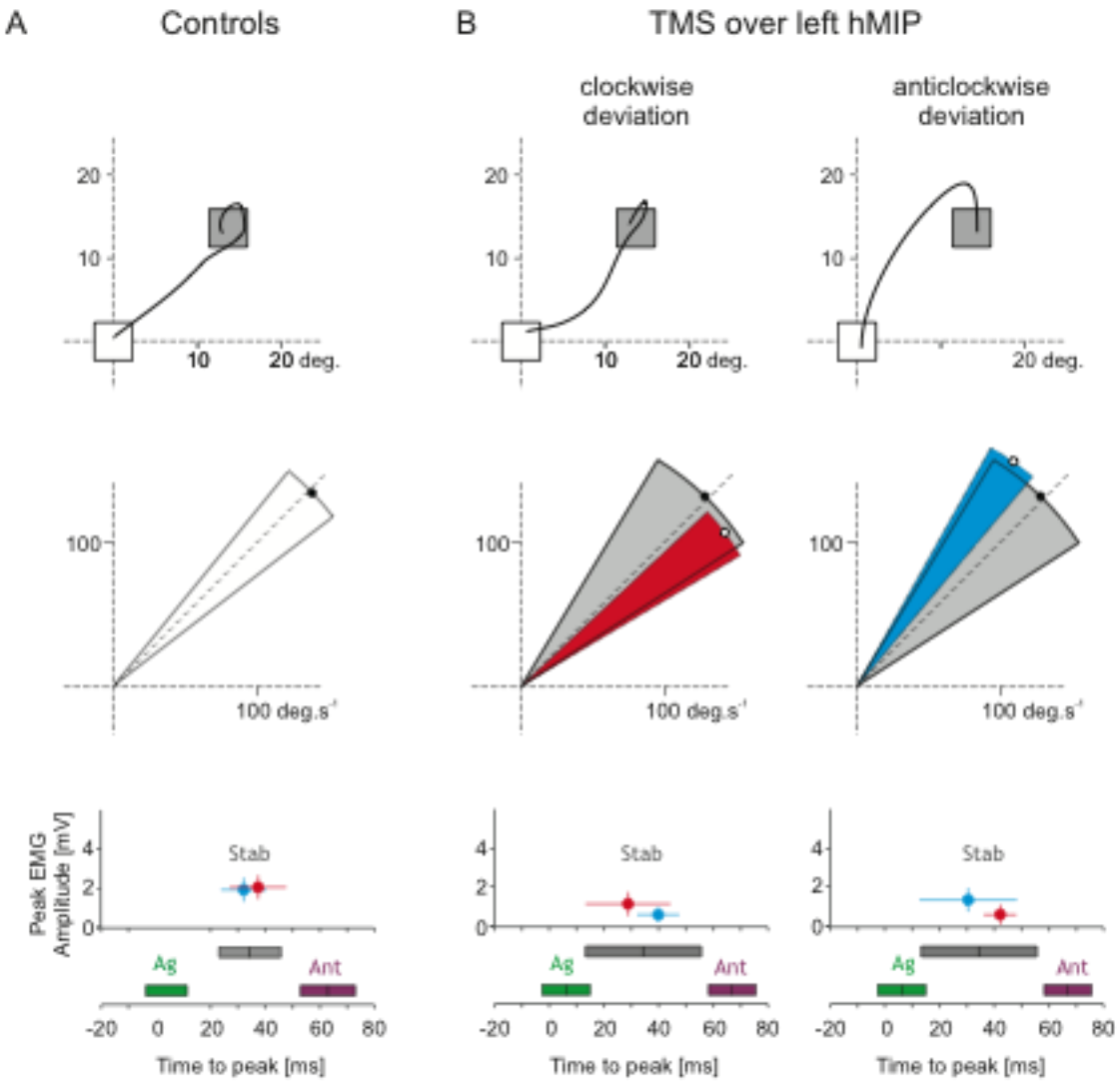
A
Controls
B
TMS over left hMIP
clockwise deviation
anticlockwise deviation
20
10
10
20 deg.
100
100 deg.s-1
Peak EMG Amplitude [mV]
4
2
0
Stab
Ag
Ant
-20
0
20
40
60
80
Time to peak [ms]

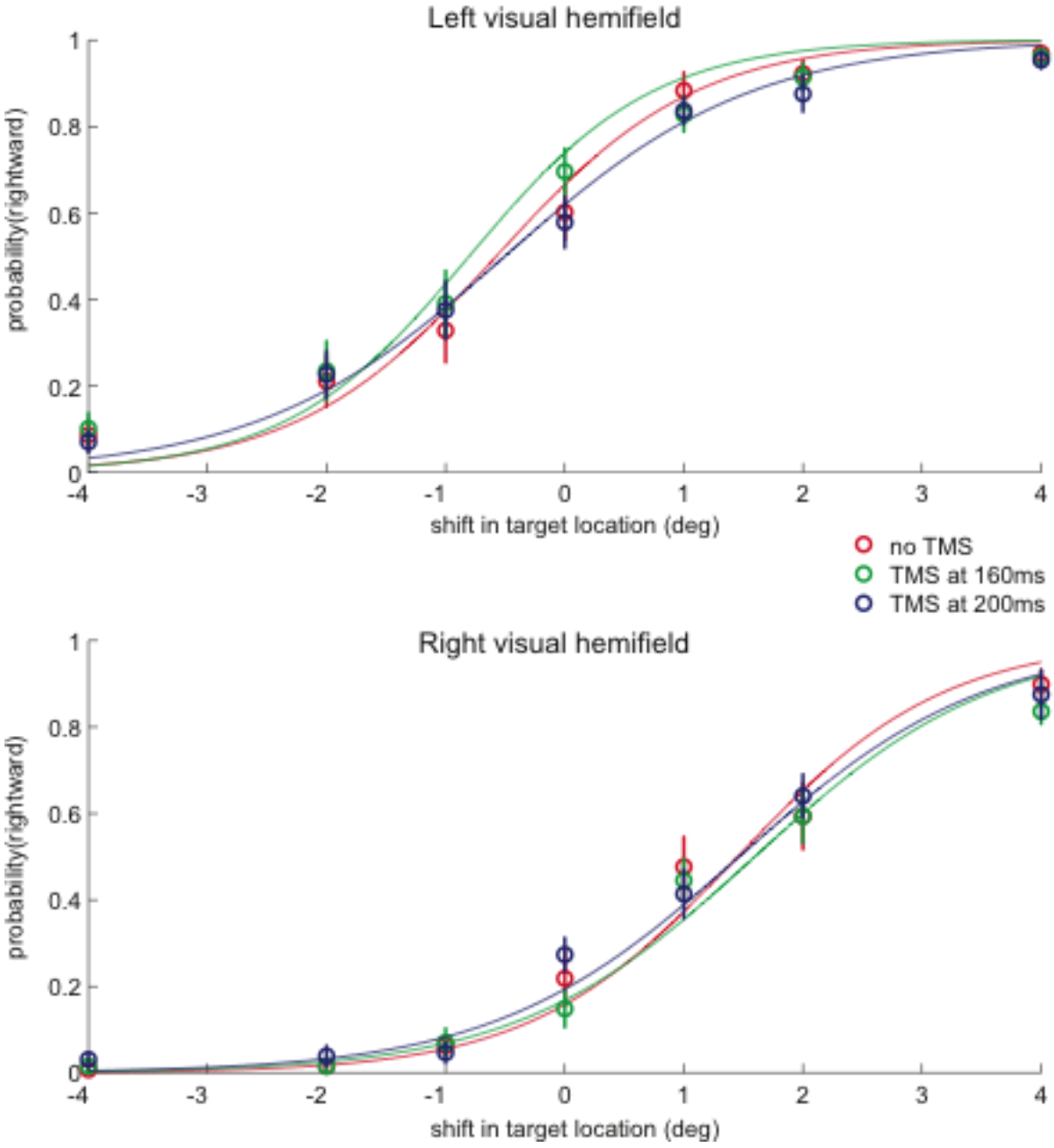
Left visual hemifield
probability(rightward)
shift in target location (deg)
no TMS
TMS at 160ms
TMS at 200ms
Right visual hemifield
probability(rightward)
shift in target location (deg)

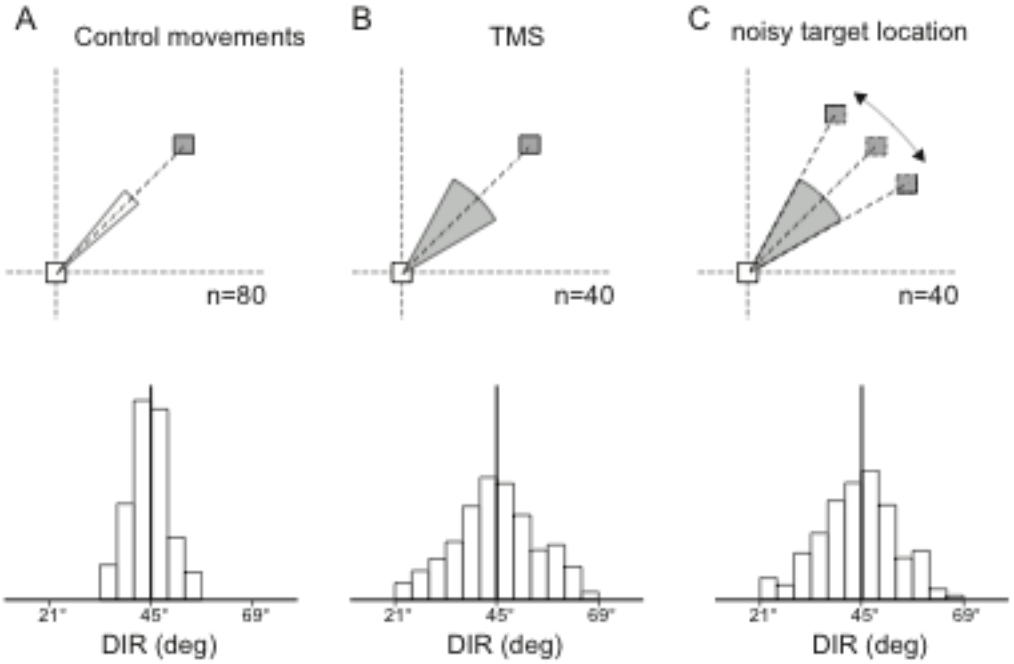
A
Control movements
n=80
21°
45°
69°
DIR (deg)
B
TMS
n=40
21°
45°
69°
DIR (deg)
C
noisy target location
n=40
21°
45°
69°
DIR (deg)

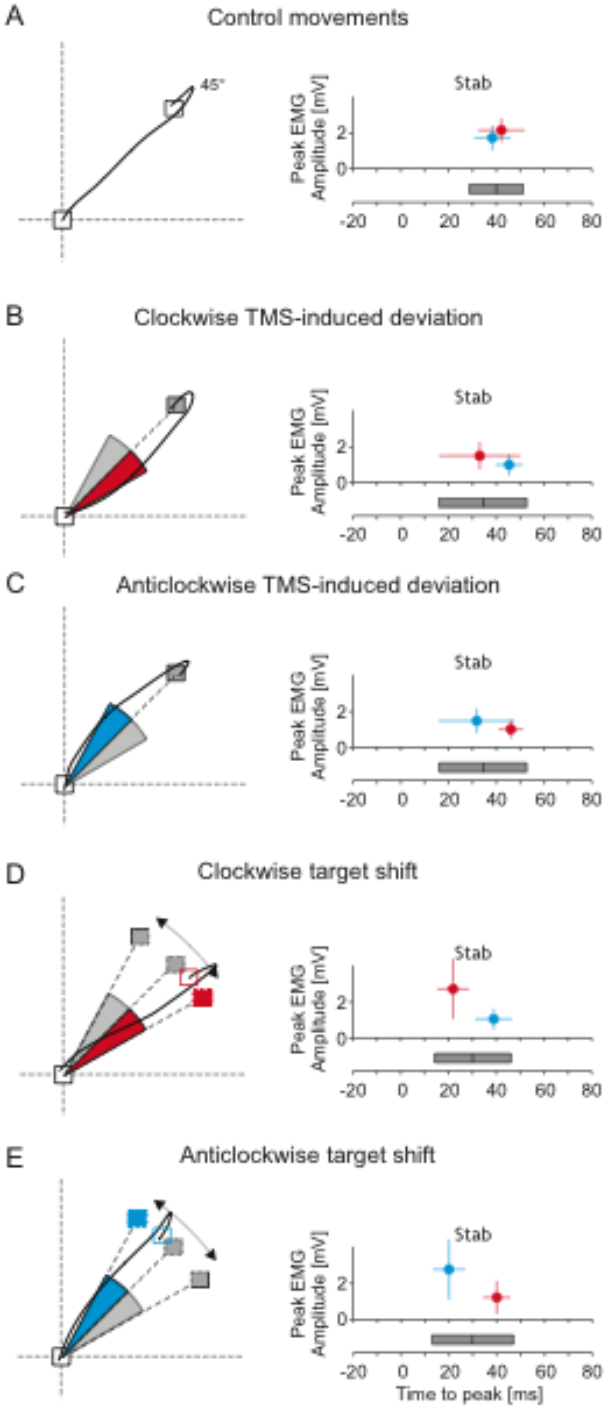
A
Control movements
45°
Stab
Peak EMG Amplitude [mV]
2
0
-20
0
20
40
60
80
B
Clockwise TMS-induced deviation
Stab
Peak EMG Amplitude [mV]
C
Anticlockwise TMS-induced deviation
Stab
Peak EMG Amplitude [mV]
D
Clockwise target shift
Stab
Peak EMG Amplitude [mV]
E
Anticlockwise target shift
Stab
Peak EMG Amplitude [mV]
Time to peak [ms]